Advances in Nano Research, *Vol. 11, No. 3 (2021) 227-237*
https://doi.org/10.12989/anr.2021.11.3.227

Synthesis, characterization, and antimicrobial activities of 3-HPAA-Alg-Chi nanoparticles

Ozgun O. Ozdemir[a] and Ferda Soyer*

Department of Molecular Biology and Genetics, Izmir Institute of Technology, Urla, 35430, Izmir, Turkey

(*Received March 20, 2019, Revised May 24, 2021, Accepted May 27, 2021*)

Abstract. Encapsulation of bioactive compounds (e.g., phenolic acids) into nanoparticles is a well-received technique in the searching for new antimicrobial agents against multidrug-resistant pathogens. Encapsulation can be a good technique to maintain the stability of phenolic acids against environmental conditions. In this study, 3-hydroxyphenylacetic acid (3-HPAA) was encapsulated into alginate-chitosan nanoparticles with the ion gelation technique. The characterization of loaded and unloaded nanoparticles was performed via dynamic light scattering, Fourier transform infrared spectroscopy, and scanning electron microscopy. According to the results, 3-HPAA loaded nanoparticles have spherical shapes with a diameter range of 40-80 nm and an average hydrodynamic diameter of 361.0 ± 69.8 nm. The loading of 3-HPAA was successfully achieved based on the Fourier transform infrared spectra and encapsulation percentage studies. The antimicrobial effect of the nanoparticles in solution forms was tested on *P. aeruginosa*, *S. epidermidis*, MRSA, and MSSA. The results demonstrated that the 3-HPAA loaded alginate chitosan nanoparticle solution showed elevated antimicrobial effect due to the pH change by treatment with 1% acetic acid, and it displayed bacteriocidal effects in a strain-specific and dose-dependent manner. Therefore, the 3-HPAA loaded alginate chitosan nanoparticle solution was produced successfully with the bacteriocidal effect against serious pathogenic bacteria.

Keywords: FT-IR; alginate-chitosan nanoparticles; antimicrobial; pathogenic bacteria; phenolic acid; *pseudomonas aeruginosa*; *staphylococci*; 3-Hydroxyphenylacetic acid

1. Introduction

Encapsulation of bioactive compounds is an attention-grabbing concept in the biomedical field nowadays since it may facilitate long-term stability and preserved therapeutic effect (Kaur *et al.* 2020, Scolari *et al.* 2020, Longuinho *et al.* 2019, Nalini *et al.* 2019). In the encapsulation process, chitosan and alginate are widely used materials since they are both easy-to-use, biocompatible and biodegradable compounds (Paques *et al.* 2014). Chitosan is a cationic polymer produced from chitin with antimicrobial properties (Jayakumar *et al.* 2010). It can be united with vitamins, minerals, oils, proteins, and biologically active natural compounds to make effective substances (Tang *et al.* 2013, Azevedo *et al.* 2012, Budnyak *et al.* 2016, Deka *et al.* 2016, Wu *et al.* 2018, Moschona and Liakopoulou-Kyriakides, 2018). Alginate is a biocompatible, water-soluble anionic polymer with low toxic properties obtained from algae (Paques *et al.* 2014).

Its property of synthesizing hydrogels in the presence of divalent cations makes it an important material for encapsulation processes (Yang *et al.* 2011). In this study, the ion gelation technique was used to encapsulate 3-hydroxyphenylacetic acid (3-HPAA) into alginate-chitosan nanoparticles. In the encapsulation process, calcium chloride ($CaCl_2$) was used as a crosslinker to produce the alginate complex with 3-HPAA (Ji *et al.* 2019). The outermost layers of the nanoparticles consist of chitosan, which was used to cover the alginate-3-HPAA complex. Because of alginate's anionic nature, coating it with cationic chitosan in the encapsulation process would result in the formation of alginate-chitosan nanoparticles by electrostatic interactions (Liu *et al.* 2018) and provide a durable coat for better structural stability. (Paques *et al.* 2014).

Pseudomonas aeruginosa, *Staphylococcus epidermidis*, and *Staphylococcus aureus* (methicillin-resistant or susceptible) are well-known nosocomial opportunistic pathogens. They result in serious infections in humans, especially in immunocompromised patients. These infections cause high morbidity and mortality worldwide. Although the infections could be treated with antibiotics, combatting these bacteria is challenging due to their existing resistance against most antibiotics in use and their ability to develop resistance against the antibiotics. Hence, the search for new agents and ways is globally ongoing against these bacteria. Many studies demonstrate the nanoparticle application result in promising antimicrobial effects on pathogenic bacteria (Vizhi *et al.* 2016, Supraja *et al.* 2017, 2018, MubarakAli *et al.* 2018, Khan *et al.* 2019). Phenolic acids are found in many plants as secondary metabolites (Hurtado-Fernandez *et al.* 2010). The anti-microbial properties of phenolic acids and the plant extracts

*Corresponding author, Ph.D., Professor,
E-mail: ferdasoyer@iyte.edu.tr
[a] Ph.D., E-mail: ozgunozdemir@iyte.edu.tr

Copyright © 2021 Techno-Press, Ltd.

ISSN: 2287-237X (Print), 2287-2388 (Online)

that contain phenolic compounds were presented in many studies (Karaosmanoglu *et al.* 2010, Gutiérrez-Larraínzar *et al.* 2012, Díaz-Gómez *et al.* 2013, Cueva *et al.* 2010). They are bioactive compounds with many beneficial effects on human health. However, their sensitivity to environmental conditions may lead to fluctuated or decreased anti-microbial effects. The encapsulation provides structural durability by decreasing the oxidation or degradation of the phenolic acids (Li *et al.* 2015). Recently, an increasing number of studies focus on phenolic compound-based antimicrobial agents (Liu *et al.* 2018, Wu *et al.* 2018). These studies demonstrate promisingly efficient results to combat the pathogenesis. The 3-hydroxyphenylacetic acid (3-HPAA) is a water-soluble, simple phenolic acid with dose-dependent antimicrobial activity on pathogenic bacteria, which was determined in our previous studies (data not shown). In the current study, we would like to show the significant antimicrobial effects of encapsulated 3-HPAA in the solution form.

Herein we report the production, physicochemical characterization, and antimicrobial effects of alginate-chitosan nanoparticles loaded with 3-HPAA (3-HPAA-Alg-Chi) in comparison to unloaded nanoparticles (Alg-Chi). To the best of our knowledge, this is the first study that shows the encapsulation of 3-HPAA in Alg-Chi nanoparticles and shows a strong antimicrobial effect on serious nosocomial bacteria, *P. aeruginosa*, *S. epidermidis*, methicillin-resistant *S. aureus* (MRSA), and methicillin-susceptible *S. aureus* (MSSA).

2. Materials and methods

2.1 Materials

Chitosan (low molecular weight, 50–190 KDa based on viscosity) (Sigma-Aldrich, product no: 448869), alginic acid sodium salt (low viscosity;) (Sigma-Aldrich, product no: 180947), calcium chloride dihydrate ($CaCl_2.2H_2O$) (Sigma-Aldrich), sodium hydroxide (NaOH) (Sigma-Aldrich), hydrochloric acid (HCl) (Sigma-Aldrich), acetic acid (Sigma-Aldrich), 3-hydroxyphenylacetic acid (Sigma-Aldrich), ethanol (Sigma-Aldrich), agar (Sigma-Aldrich) and tryptic soy broth (Merck) were purchased commercially.

2.2 Synthesis of nanoparticles

Alg-Chi nanoparticles were synthesized based on the protocol of Azevedo *et al.* (2014) with a slight modification (25 mM $CaCl_2$ usage rather than 18 mM) under sterile conditions (Azevedo *et al.* 2014). Briefly, sodium alginate was dissolved in double-distilled water (ddH_2O) with a final concentration of 0.63 mg/ml for each type of nanoparticle. The pH of the solution was adjusted to pH 4.9 with 1M HCl. For the phenolic acid loaded nanoparticles, 3-HPAA with a final concentration of 25 mg/ml was dissolved in an alginate solution. Chitosan was dissolved in 1% (v/v) acetic acid with a final concentration of 0.4 mg/ml for each type of nanoparticles, and pH was adjusted to pH 4.6 with 1M NaOH. Then, 7.5 ml calcium chloride dihydrate (from 25 mM stock solution) was added into alginate solution with 0.125 ml/min flow rate at 20.000 rpm continuous stirring via Ultra-Turrax (Ika, T-18). The chitosan solution was added into each pre-gel (alginate-calcium chloride solutions with or without 3-HPAA) with 0.278 ml/min flow rate in a volume ratio of 5:1 (alginate:chitosan) at 600 rpm continuous stirring. Then, nanoparticle solutions were stirred at 600 rpm for 20 more minutes. They were stored at 4°C. Prior to use in each experiment, the nanoparticles were vortexed for 30 seconds and sonicated for 30 minutes at 4°C.

2.3 Characterization of nanoparticles

2.3.1 Determination of particle size and polydispersity Index (PDI)

The size distribution (by number distribution) and polydispersity index (PDI) of all sonicated nanoparticles were determined by dynamic light scattering (DLS) by Zetasizer (Nanoplus 3 Zeta/nanoparticle analyzer, Micro-meritics) via Nanoplus version 5.22/3 software, with a scattering angle of 165º and repetition of 2, at 25°C. Each sample was placed in disposable DLS cuvettes in 3 ml volume for each measurement. Average values and standard deviations were calculated by Microsoft Excel software.

2.3.2 Fourier transform infrared spectrometry (FT-IR) analysis

The infrared spectra of all compounds were recorded via FT-IR spectrometer (PerkinElmer Spectrum 2) in the mid-infrared (4000-650 cm^{-1} wavenumber) range by transmittance values at room temperature. The spectrometer was equipped with a deuterated tri-glycine sulfate (DTGS) detector and a horizontal attenuated total reflectance (HATR) sampling accessory (ZnSe crystal). In each measurement, the number of scans was 20, and the resolution was set to 4 cm^{-1}. Before FT-IR measurements, each nanoparticle solution was freeze-dried in a lyophilizer (Labconco-Freezone) for 24 hours. The collection of background spectra was done before measurement. Each sample (produced nanoparticles (Alg-Chi and 3-HPAA-Alg-Chi), chitosan, alginate, and 3-HPAA) was placed on the instrument's crystal and then compressed by the metal arm. After the stable force gauge was observed, the spectra data were collected by Spectrum software (Version 10.4.3). The ZnSe crystal was cleaned with isopropyl alcohol before the analysis of each sample.

2.3.3 Morphology determination

Sonicated 3-HPAA-Alg-Chi nanoparticles were centrifuged at 18.000 x g for 30 minutes at 4ºC. They were diluted 2-fold by resuspending the pellet in ddH_2O. After the 15 seconds vortex and 5 minutes of sonication, 10 µl of each sample was spread on aluminum foil and dried at 37ºC for 30 minutes. Then, samples were placed on double-sided carbon bands on metal grids and covered with gold for 2 minutes. They were investigated under SEM (Philips XL 30) with 100,000X magnification.

2.4 Encapsulation percentage of 3-HPAA into nanoparticles

To calculate the encapsulation percentage, firstly, the wavelength and standard graph of 3-HPAA were determined. UV-spectrum scanning in the range of 200-400 nm wavelength (Thermo Multiscan) was used for wavelength determination. The standard graph was then plotted based on the absorbance values measured spectrophotometrically at the specific wavelength determined by UV-spectrum scanning (270 nm). The absorbance (nm) versus 3-HPAA concentration (mg/ml) were plotted, and the best fit linear equation was obtained.

The sonicated 3-HPAA loaded nanoparticle solution was centrifuged at 18000 x g for 30 minutes. The supernatant was measured spectrophotometrically at the determined wavelength (270 nm). The supernatant phenolic acid concentration was calculated using the equation of the standard graph based on the absorbance values. The averages and standard deviations were determined by Microsoft Excel software.

2.5 Antimicrobial effects of nanoparticle solutions

The antimicrobial effect of 3-HPAA loaded Alg-Chi nanoparticle solution was tested on nosocomial bacteria *Pseudomonas aeruginosa* (ATCC 27853), *Staphylococcus epidermidis* (ATCC 35984), methicillin-resistant *Staphylococcus aureus* (MRSA) (N315 type II SCC*mecA*), and methicillin-sensitive *Staphylococcus aureus* (MSSA) (ATCC 29213) by agar diffusion and spectrophotometric measurements. The single colonies of each bacterium were inoculated into tryptic soy broth (TSB) and incubated at 37°C for 18 hours to obtain overnight bacterial cultures in each study.

In the antimicrobial effect determination studies, nanoparticle solutions were treated with acetic acid (1% (v/v) final concentration, in ddH_2O) for the release of 3-HPAA. This treatment was carried out at 4°C for 24 hours and 72 hours before their use for agar diffusion tests and 24 hours for spectrophotometric growth measurements.

2.5.1 Agar diffusion tests

In agar diffusion studies, 100 µl volume of each bacterium from overnight culture was spread on tryptic soy agar (TSA) and allowed to be absorbed by agar for 1 hour at room temperature. The nanoparticle solutions, acetic acid solution (1%), and ethanol solution (80%) were dropped on plates in 15 µl volume according to the template in Fig. 1. In this figure, each number represents the region of the solution name in the adjacent box as I: 80% ethanol, II: 1% acetic acid, III: Alg-Chi nanoparticles, IV: 1% acetic acid-treated Alg-Chi nanoparticles, V: 3-HPAA-Alg-Chi nanoparticles, VI: 1% acetic acid-treated 3-HPAA-Alg-Chi nanoparticles (Fig. 1). The incubation was carried out at 37°C overnight.

2.5.2 Bacterial growth determination

The antimicrobial effect of nanoparticle solutions on bacterial growth was determined by inoculating overnight cultures with the 10^6 cfu/ml final concentration into TSB containing 10% or 20% final volumes (v/v) nanoparticle solutions. The effect of 1% acetic acid in ddH_2O on bacterial growth was simultaneously tested. Optical densities (OD) of bacteria were measured spectrophotometrically at 600 nm at the 0^{th} and 24^{th} hours of growth. The graphs were plotted, and standard deviations were calculated by Microsoft Excel software. After 24 hours of incubation, the cell viabilities of the treated cultures were determined via enumeration studies by spread plating on TSA plates. The plates were incubated overnight at 37°C, and bacterial amounts were calculated in cfu/ml.

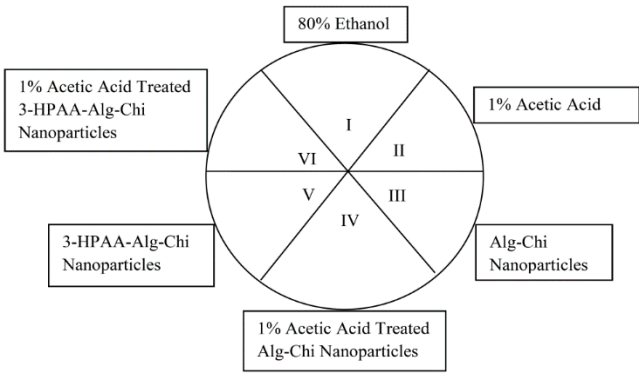

Fig. 1 The template of regions on which the solutions were dropped on TSA plates in agar diffusion tests

3. Results and discussion

3.1 Characterization and encapsulation percentage

3.1.1 Average particle size and polydispersity index (PDI)

The DLS was used in the determination of average size and PDI of nanoparticle solutions. The results indicated the increment in the average size of Alg-Chi nanoparticles, which indicates the successful encapsulation of 3-HPAA. The size distribution profile of nanoparticles in Fig. 2 clearly demonstrated that the shift of the peak of 3-HPAA-Alg-Chi (black peak) was further to the right than Alg-Chi (blue peak) nanoparticles, which shows they have bigger average sizes than those of Alg-Chi (blue peak) nanoparticles. In addition, the occurrence of a single peak for each nanoparticle solution revealed the perfect uniformity of the particle sizes (Mohammadi *et al.* 2016). Relatedly, the average size of Alg-Chi and 3-HPAA-Alg-Chi were observed as 278.8 ± 12.4 nm and 361.0 ± 69.8 nm, respectively (Table 1). According to these diameters, Alg-Chi nanoparticles have smaller diameters than those of 3-HPAA-Alg-Chi, and the size distribution of Alg-Chi is narrower (with ± 12.4 standard deviation) than 3-HPAA-Alg-Chi (with ± 69.8). This situation shows that, although the nanoparticle synthesis protocol supports the production of homogeneous nanoparticles, the loading with 3-HPAA results in a slight decrease in the particles' homogeneity.

Another important parameter for particle size distribution is the polydispersity index (PDI) value. The

particles with smaller PDI values (PDI < 1) have narrow size distributions, and relatedly, they are more homogeneous in size (Liu *et al.* 2018, Qi *et al.* 2004). The PDI values were recorded as 0.22 for Alg-Chi and 0.23 for 3-HPAA-Alg-Chi nanoparticles (Table 1). Therefore, they both could be accepted as homogenous particles with similar homogeneity patterns.

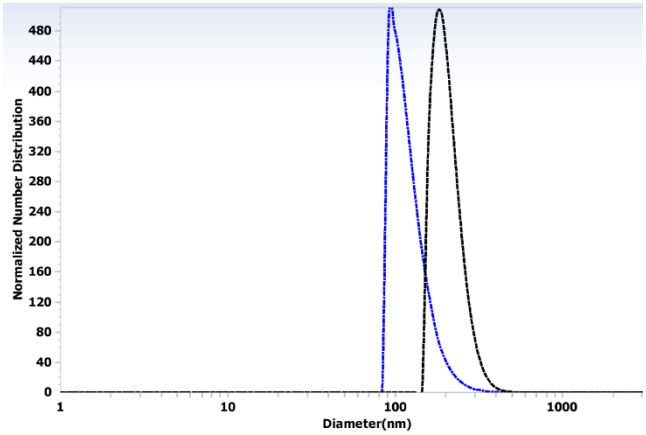

Fig. 2 Normalized number distribution of Alg-Chi and 3-HPAA Alg-Chi nanoparticles (Black peak: 3-HPAA-Alg-Chi, Blue peak: Alg-Chi)

Table 1 Comparison of average hydrodynamic diameters (nm) and polydispersity index (PDI) values of Alg-Chi and 3-HPAA-Alg-Chi nanoparticles via DLS

Sample Name	PDI	Average hydrodynamic diameters (nm)
Alg-Chi Nanoparticles	0.22	278.8±12.4
3-HPAA Alg-Chi Nanoparticles	0.23	361.0±69.8

3.1.2 Fourier transform infrared spectra

The determination of physicochemical properties of the Alg-Chi and 3-HPAA-Alg-Chi nanoparticles was performed via FTIR analyses. The changes in wavenumbers of peaks were determined in the spectra of the compounds, especially in the region between 1700- 650 cm-1 wavenumbers (Fig. 3). In Fig. 3, the spectrum of each compound was indicated with a different color: 3-Hydroxyphenylacetic Acid (3-HPAA) (pink), Chitosan (Chi) (yellow), Alginate (Alg) (purple), Alginate-Chitosan Nanoparticles (Alg-Chi) (grey), and 25 mg/ml 3-Hydroxyphenylacetic Acid Loaded Nanoparticles (3-HPAA-Alg-Chi) (orange).

The FTIR spectra of the Alg-Chi and 3-HPAA-Alg-Chi comparison indicates that there were hydroxyl groups in each compound depending on the peak complexes at 3264 and 3241 cm^{-1} for Alg-Ci and 3-HPAA-Alg-Chi, respectively. These arouse from oxial O-H and N-H stretching of Chi (3288 cm^{-1}) and O-H stretching of Alg (3240 cm^{-1}) (Wu *et al.* 2018). In addition, since the 3-HPAA loading was achieved, the shift of the peak of Alg-Chi (3264 cm^{-1}) to the lower wavenumbers in 3-HPAA-Alg-Chi (3241cm^{-1}) was seen (Wu *et al.* 2018). The CH stretching of 3-HPAA at 2965 cm^{-1} (Barrera-Necha *et al.* 2018) was disappeared in 3-HPAA-Alg-Chi, which also shows the loading of 3-HPAA.

Since an electrostatic interaction occurs between the

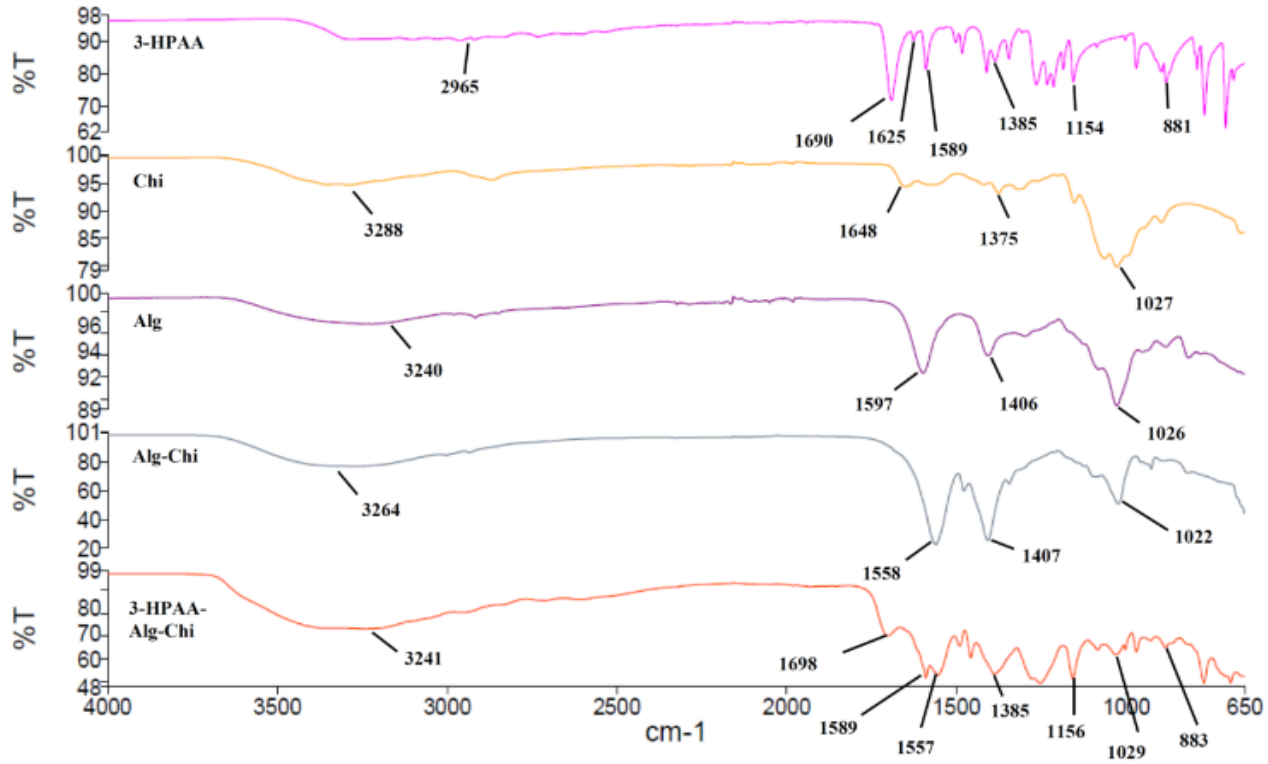

Fig. 3 Comparison of the FT-IR Spectra analysis of the compounds in mid-IR

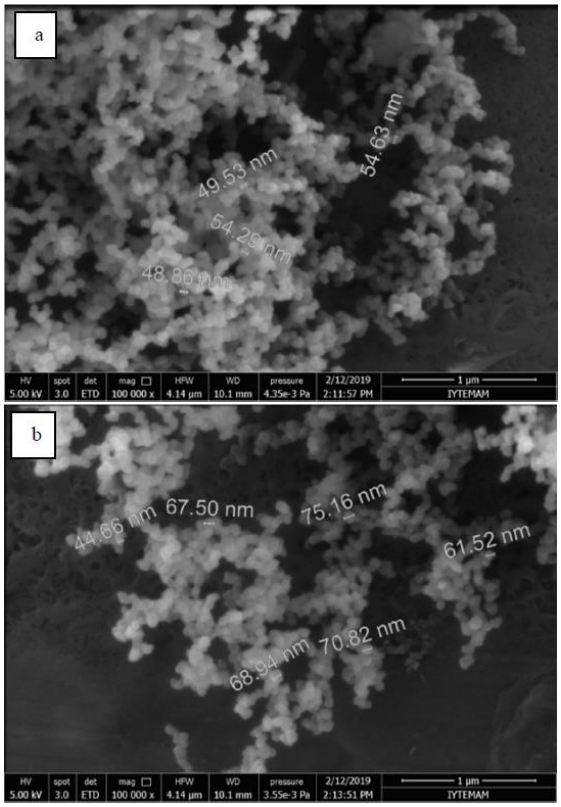

Fig. 4 Morphologies (a) and size range (b) of 3-HPAA-Alg-Chi nanoparticles under scanning electron microscopy

amine group of Chi (1648 cm^{-1}) and the carboxylate group of Alg (1597 cm^{-1}), the peak which was recognized at 1558 cm^{-1} in Alg-Chi, shifted to higher wavenumber (1698 cm^{-1}) in 3-HPAA-Alg-Chi (Wu *et al.* 2018). The symmetric stretching in carboxylic acid groups of Alg and Chi creates the peaks at 1404 cm^{-1} in Alg-Chi (Wu *et al.* 2018). In 3-HPAA-Alg-Chi, this peak shifts to 1385 cm^{-1} because of 3-HPAA loading. The peak at 1022 cm^{-1} in Alg-Chi shifted to 1029 cm^{-1} in 3-HPAA-Alg-Chi. Similar bands were detected in chitosan and alginate at 1027 cm^{-1} and 1026 cm^{-1} for chitosan and alginate, respectively. These wavenumbers correspond to stretching vibrations of C-O-C of the polysaccharide (Liu *et al.* 2018). The peak at 1154 in 3-HPAA matches the asymmetric stretching of the C-O-C bridge (Mladenovska *et al.* 2007), which was shifted to 1156 in 3-HPAA-Alg-Chi because of the loading of 3-HPAA. Similarly, the peak of 3-HPAA at 881 $cm^{-1,}$ which might correspond to the aromatic ring (Barrera-Necha *et al.* 2018), shifted to 883 cm^{-1} in 3-HPAA-Alg-Chi. Two characteristic peaks of 3-HPAA, 1589 and 1385 cm-1, were also determined in the FTIR of 3-HPAA-Alg-Chi nanoparticles, which suggests the 3-HPAA loading into the nanoparticles (Kaur *et al.* 2020; Liu *et al.* 2018). To sum up, the physicochemical properties of synthesized nanoparticles were similar except the mentioned shifts in peaks of 3-HPAA-Alg-Chi caused by successful loading of 3-HPAA.

3.1.2 Scanning electron microscopy

The scanning electron micrographs of 3-HPAA-Alg-Chi nanoparticles indicated that their shapes were spherical (Figs. 4(a)-(b)). The nanoparticles were recognized as slightly agglutinated since chitosan-based particles have a natural property of generating agglomerates. This situation could be explained, "due to the van der Walls attractive forces dominating over repulsive forces between the particles" (Jamil *et al.* 2016). The diameters of nanoparticles that could be detected with individual boundaries were measured by SEM instrument. The nanoparticles were observed as homogenous (Fig. 4(a)), and the diameters in a range of 40-80 nm (Fig. 4(b)). In DLS analyses, the average diameters were measured as 278.8±12.4 and 361.0±69.8 nm for Alg-Chi and 3-HPAA-Alg-Chi nanoparticles, respectively. These higher diameters were expected in DLS since the technique measures the hydrodynamic diameters (Krausz *et al.* 2015) of the nanoparticles.

Although our results related to spherical nanoparticles' production were similar to Azevedo *et al.* (2014), they have differences in the homogeneity (Azevedo *et al.* 2014). The nanoparticles of their study were not homogenous under transmission electron microscopy (TEM), while in our study, it was found that they were homogenous according to SEM images and PDI values. These differences might be the result of the increased concentration of calcium chloride ($CaCl_2$) used in this study and the nature of the encapsulated compounds.

3.2 Encapsulation percentage

To calculate the encapsulation percentage of 3-HPAA into nanoparticles, the equation (Eq. (1) of the standard graph (R2 = 0.996) of 3-HPAA was used (Fig. 5(b)) plotted with absorbance measured at 270 nm (Fig. 5(a)). The y value of the equation corresponds to the average absorbance value of the supernatant, and the x value corresponds to the concentration of phenolic acid in the supernatant at the specific wavelength of 3-HPAA (Fig. 5 (a)). The equation of the standard graph of 3-HPAA was:

$$y = 10.665x - 0.005 \quad (1)$$

Since the centrifugation of the nanoparticle solution provided not only the harvest of the nanoparticles but also the removal of the excess polymers and impurities, the supernatant contains the 3-HPAA that could not be encapsulated into nanoparticles. The calculation of encapsulation percentage for 3-HPAA into nanoparticles was carried out with the Eq. (2):

$$Encapsulation\ percentage = 100 - [\left(\frac{Supernatant\ phenolic\ acid\ concentration}{Total\ phenolic\ acid\ concentration}\right) * 100] \quad (2)$$

According to the absorbance results and calculations with standard graph equation (Eq. (2)), the average concentration of 3-HPAA in the supernatant was 0.28 (±0.017) mg/ml. The average encapsulation percentage of 3-HPAA into nanoparticles was calculated as 99.9% (±0.04), which indicates a very high encapsulation.

Calcium chloride, which is used as the crosslinker for alginate, is an important parameter in the homogeneity, size,

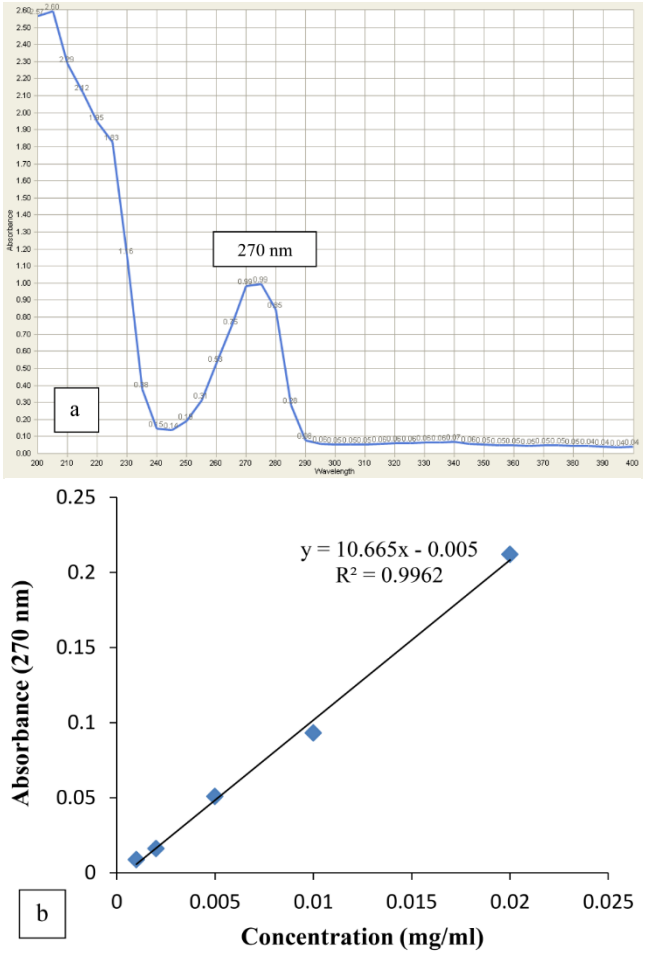

Fig. 5 The UV-spectrum and standard graph of 3-HPAA. a) Significant peak of 3-HPAA in UV-spectrum analysis x: Wavelength (200-400 nm); y: Absorbance b) The standard graph and the equation of 3-HPAA x: Concentration (mg/ml); y: Absorbance (270 nm)

and loading percentage of nanoparticles. When $CaCl_2$ was used in higher concentrations in the production process, the average sizes and PDI values decrease, and loading percentages increase (Wu *et al.* 2018). In the study of Wu *et al.* (2018), the concentrations of $CaCl_2$ were evaluated in 1 mM, 3 mM, and 5 mM in encapsulation of lysozyme into Alg-Chi nanoparticles. When considering the small average size, low PDI, and high encapsulation percentage, the best result among these concentrations was found in the usage of 5 mM $CaCl_2$. They suggested that the elevated calcium ion concentration results in fine pores and compact gelation of the polymers due to the increased cross-linking properties (Wu *et al.* 2018). Since $CaCl_2$ was used in 25 mM concentration in our protocol, the higher molarity of $CaCl_2$ provided the production of smaller and more homogenous nanoparticles with very high loading percentages.

In a similar study, phenolic acid encapsulations (rosmarinic acid, protocatechuic acid, or 2,5-dihydroxybenzoic acid) into chitosan nanoparticles were performed with both high and low molecular weight chitosan (Madureira *et al.* 2015). Our results could be compared with the low molecular weight chitosan results of Madureira *et al.* (2015) since low molecular weight chitosan was used in our study (Madureira *et al.* 2015). Their percent encapsulation results were between 60-90%, which is also a high degree of encapsulation. Likewise, the encapsulation percentage was 99.9% (±0.04) in our study. The increase in encapsulation percentage might be due to using alginate to entrap the phenolic acids before chitosan covering. In addition, we used $CaCl_2$ as a crosslinker rather than the tripolyphosphate that they used, which might change the conditions of entrapment. Another reason for achieving a high encapsulation percentage in our study might be related to the simpler structure and different physicochemical properties of 3-HPAA than these of rosmarinic acid, protocatechuic acid, or 2,5-dihydroxybenzoic acid. Briefly, it could be speculated that the phenolic acid entrapment into the alginate with $CaCl_2$ crosslinker before chitosan coating resulted in the highest phenolic acid encapsulation.

3.3 Antimicrobial effects of nanoparticles

The antimicrobial effects of 3-HPAA Alg-Chi nanoparticles on nosocomial bacteria were clearly demonstrated by agar diffusion tests, spectrophotometric measurements, and viable counts.

3.3.1 Inhibition zones of nanoparticles

The results of the antimicrobial effect of the 3-HPAA loaded nanoparticle (3-HPAA-Alg-Chi) solutions and unloaded nanoparticle solutions were shown for *P. aeruginosa* in Figs. 6(a-1)-(a-2), for *S. epidermidis* in Figs. 6(b-1)-(b-2), for MRSA in Figs. 6(c-1)-(c-2) and for MSSA in Figs. 6(d-1)-(d-2) in duplicates. Since the acetic acid (1%, v/v final concentration) treatment of nanoparticles facilitated the release of 3-HPAA, the effect of 1% acetic acid was also tested. In Fig. 6, the numbers I, II, III, IV, V, and VI show the regions of solutions 80% ethanol, 1% acetic acid, Alg-Chi, acetic acid-treated Alg-Chi (null), 3-HPAA-Alg-Chi and acetic acid-treated 3-HPAA-Alg-Chi, respectively (Fig. 6). There were no inhibition zones in the Alg-Chi or acetic acid regions, while clear zones were observed in the 3-HPAA-Alg-Chi regions (Fig. 6). This result indicates that the antimicrobial effect was related to 3-HPAA, not related to the presence of either Alg-Chi or acetic acid.

In the study of Liu *et al.* (2018), the antimicrobial effects of alginate-chitosan nanoparticles were tested as well as ε-polylysine loaded alginate-chitosan nanoparticles on *E. coli*, *B. subtilis*, *S. aureus* and *M. luteus* (Liu *et al.* 2018). In agreement with our results, even though the ε-polylysine loaded alginate-chitosan nanoparticles produced significant inhibition zones, unloaded alginate-chitosan nanoparticles did not produce any inhibition zones.

The inhibition zone patterns produced by nanoparticles treated with acetic acid for 24 hours and 72 hours were similar for each bacterium. Therefore, the antimicrobial properties of the 3-HPAA-Alg-Chi solution could be achieved by 24 hours of acetic acid treatment prior to usage. Besides, even after 72 hours of acetic acid treatment, the antimicrobial effect was maintained. Surprisingly, the antimicrobial effect of the 3-HPAA-Alg-Chi solution was recognized even without acetic acid treatment on *P.*

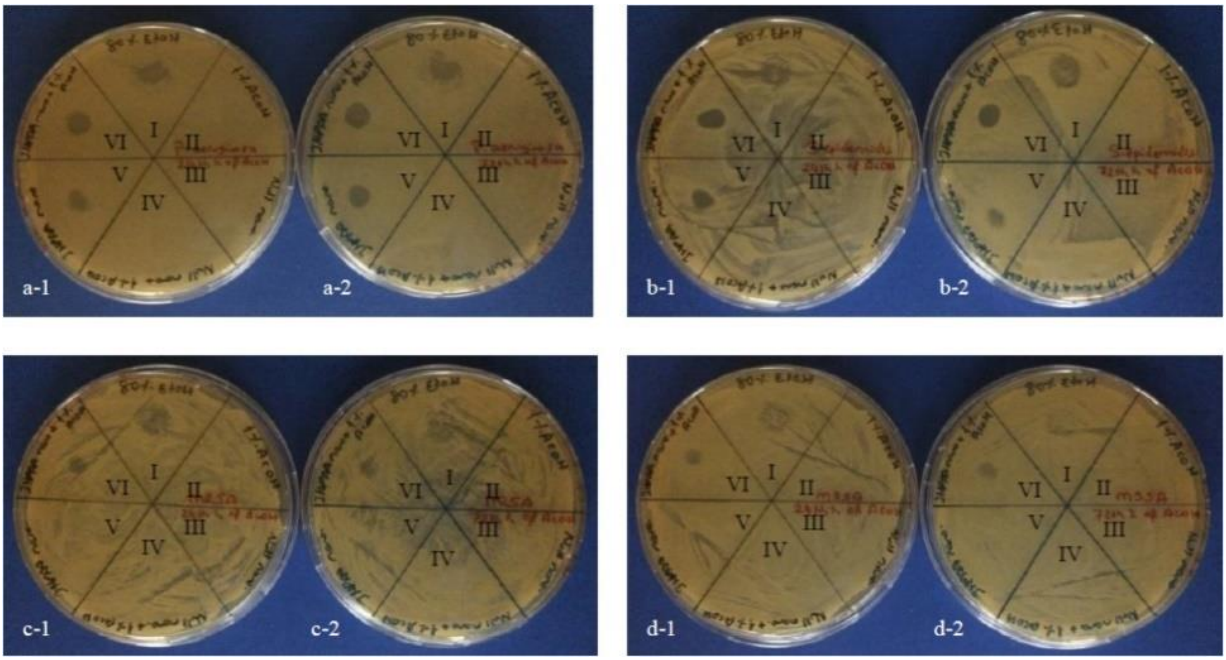

Fig. 6 Effect of Alg-Chi and 3HPAA-Alg-Chi solutions with 1% acetic acid treatment for 24 hours (a-1, b-1, c-1, d-1) or 72 hours (a-2, b-2, c-2, d-2)

aeruginosa and *S. epidermidis*. Since the Alg-Chi nanoparticle solution had no zones, the interactions of 3-HPAA with alginate and chitosan might provide an increased antimicrobial effect on *P. aeruginosa* and *S. epidermidis*. Besides, in both bacteria, the acetic acid-treated 3-HPAA-Alg-Chi solution produced more clear and bigger diameters of the inhibition zones than those of nontreated 3-HPAA-Alg-Chi. This situation was expected since acetic acid treatment provided the release of 3-HPAA from the nanoparticles, resulting in a higher antimicrobial effect of the 3-HPAA-Alg-Chi solution.

In contrast to the results of *P. aeruginosa* and *S. epidermidis*, in the regions of the 3-HPAA-Alg-Chi solution without acetic acid treatment, no inhibition zones were observed in MRSA and MSSA. In our preliminary studies (data not shown), the application of 25 mg/ml, 3-HPAA on MRSA and MSSA did not produce any inhibition zone. However, the acetic acid-treated 3-HPAA-Alg-Chi solution produced inhibition zones on both MRSA and MSSA. These results demonstrate the synergistic effect of 3-HPAA-Alg-Chi and acetic acid, as well as the enhancement of the antimicrobial effect of 3-HPAA by the encapsulation process. Similarly, the enhancement of the antimicrobial effect of the agents after encapsulation was presented in the studies of Jamil *et al*. (2015, 2016) for *Klebsiella pneumoniae* and *Pseudomonas aeruginosa* (Jamil *et al.* 2015) and MRSA and *E. coli* (Jamil *et al.* 2016). In 2015, they produced cephalosporin loaded chitosan nanoparticles (nanoantibiotics) and applied them on multidrug-resistant *Klebsiella pneumoniae* and *Pseudomonas aeruginosa*. The larger inhibition zones were observed with the increasing concentrations of drugs in nanoantibiotics, while the antibiotics only did not cause any inhibition zone production (Jamil *et al*. 2015). They also produced cardamom essential oil loaded chitosan nanoparticles and tested them on MRSA and *E. coli* in another study (Jamil *et al*. 2016). In the growth measurements of MRSA and *E. coli*, cardamom essential oil had no inhibition effect, while chitosan nanoparticles loaded with cardamom oil completely inhibited the growth of both pathogens. Liu *et al.* (2018) were also found that the encapsulation of ε-polylysine loaded alginate-chitosan nanoparticles showed a three-fold increase in antimicrobial activities than free ε-polylysine (Liu *et al.* 2018) on *E. coli*, *B. subtilis*, *S. aureus*, and *M. luteus*. Our results agreed with all these studies showing the increase of antimicrobial properties of bioactive compounds after encapsulation.

3.3.2 The effect of 3-HPAA-Alg-Chi on bacterial growth in broth

The antimicrobial effects of nanoparticle solutions (treated with 1% (v/v) final concentration of acetic acid for 24 hours)) on the growth of all tested bacteria were presented in Fig. 7. In each graph, the colors of lines correspond to the bacterial growth in the presence of the following: Blue line: Alg-Chi; red line: 3-HPAA-Alg-Chi; green line: 1% acetic acid and purple line: control bacteria (containing only media) (Fig. 7). *P. aeruginosa* growth was inhibited by all 3-HPAA-Alg-Chi, Alg-Chi, and 1% acetic acid solutions with the10% (v/v) application (Fig. 7(a)). However, *S. epidermidis* growth was fully inhibited by only 3-HPAA-Alg-Chi solution (Fig. 7(b)). Although the significant antimicrobial effects were achieved, a more important concept is the cell viability for antimicrobial agents to combat bacterial infections. Each tested solution showed more than 95% growth inhibition on *P. aeruginosa* by spectrophotometric measurements. However, viable count results revealed that the only 3-HPAA-Alg-Chi solution resulted in no survivors on *P. aeruginosa* among the solutions tested in 10% (v/v) final concentration

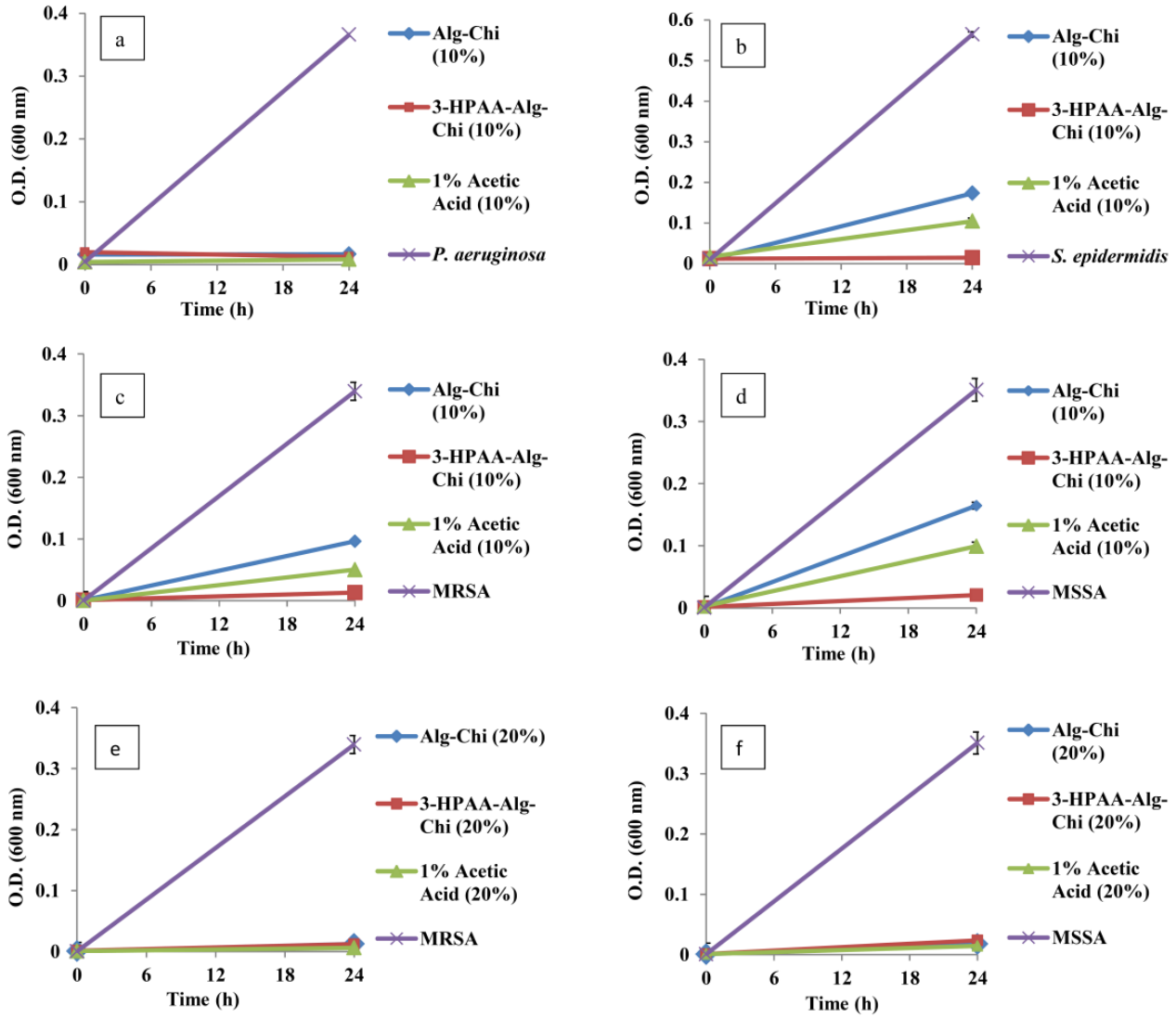

Fig. 7 The antimicrobial effects of the nanoparticles and 1% acetic acid with 10% final concentration (a, b, c, d) and 20% final concentration (e, f) on bacterial growth of *P. aeruginosa* (a), *S. epidermidis* (b), MRSA (c, e) and MSSA (d, f)

application (Table 2).

Although the usage of 20% (v/v) final concentration of all 3-HPAA-Alg-Chi, Alg-Chi, and acetic acid solutions inhibited the growth of MRSA and MSSA, only the 3HPAA-Alg-Chi solution displayed bacteriocidal effects (no survivors) on these bacteria (Figs. 7 (e)-(f) and Table 2). The usage of 20% (v/v) final concentration of 1% (v/v) acetic acid caused a significant antimicrobial effect on MRSA and MSSA. However, this result seems contrary to our results of acetic acid treatment in agar diffusion tests. There are two important parameters to consider when evaluating these results which are the bacterial load and the dose-dependent nature of the antimicrobial agents. Likewise, in the study of Jamil *et al.* (2015), it was also found that agar diffusion and broth assays showed different results in terms of the antimicrobial effect of the cefazolin-loaded chitosan nanoparticles (nanoantibiotics) (Jamil *et al.* 2015). When the lowest tested concentration in the agar diffusion tests was used in the broth assays, it showed much higher antimicrobial activity due to the bacterial load, similar to our acetic acid application results of agar diffusion and viable cell count.

In the case of *Staphylococci*, the percent inhibitions of 3-HPAA-Alg-Chi solution (in 10% (v/v) application) had the highest percent inhibitions among the all tested solutions with 97%, 96%, 94% for *S. epidermidis*, MRSA, and MSSA, respectively (Table 2). Although growth inhibitions were detected in all tested *Staphylococci*, the bacteriocidal effect was observed only on *S. epidermidis* when 10% (v/v) 3-HPAA-Alg-Chi solution was applied (Figs. 7 (b)-(d) and Table 2). On the other hand, the usage of 20% (v/v) 3-HPAA-Alg-Chi solution was required for bacteriocidal effects on MRSA and MSSA (Table 2). All of our results demonstrate that the 3-HPAA, a very important constituent for the antimicrobial property of produced nanoparticle solution, displayed its antimicrobial effects even in an increased manner after encapsulation.

Madureira *et al*. (2015) observed that the growth inhibitions of chitosan encapsulated rosmarinic acid (RA), protocatechuic acid (PA), and the 2,5-dihydroxybenzoic

Table 2 Percent growth inhibitions and viable cell counts of bacteria in the presence of nanoparticle solutions with 10% or 20% (v/v) final concentration applications

Solution concentrations (v/v)	Bacteria	Solutions	Percent Growth Inhibition (%)	Cell viability (cfu/ml)
10% (v/v)	*P. aeruginosa*	Alg-Chi	95	2×10^7
		3-HPAA Alg-Chi	97	No survivors
		Acetic acid (1%)	98	2×10^7
	S. epidermidis	Alg-Chi	69	6×10^7
		3-HPAA Alg-Chi	97	No survivors
		Acetic acid (1%)	82	3×10^7
	MRSA	Alg-Chi	72	3×10^7
		3-HPAA Alg-Chi	96	1×10^6
		Acetic acid (1%)	85	9×10^6
	MSSA	Alg-Chi	55	8×10^7
		3-HPAA Alg-Chi	94	5×10^6
		Acetic acid (1%)	73	1×10^7
20% (v/v)	MRSA	Alg-Chi	96	1×10^6
		3-HPAA Alg-Chi	96	No survivors
		Acetic acid (1%)	98	1×10^6
	MSSA	Alg-Chi	95	5×10^6
		3-HPAA Alg-Chi	94	No survivors
		Acetic acid (1%)	96	5×10^6

acid (DHBA) on various pathogenic bacteria were between 60-90% (Madureira *et al.* 2015). In our results, similarly, 3-HPAA-Alg-Chi solution displayed different levels of antimicrobial effect on different bacteria. The 10% (v/v) final concentration of the solution was enough for bacteriocidal effect for *P. aeruginosa* and *S. epidermidis*, while 20% was required for MRSA and MSSA. This situation might show that the antimicrobial effects of phenolic compounds are strain-specific and dose-dependent.

It can be concluded that the required concentration for the bacteriocidal effect of the 3-HPAA-Alg-Chi solution was 10% (v/v) on *P. aeruginosa* and *S. epidermidis* while it was 20% (v/v) on MRSA and MSSA. The bacteriocidal effect of the 3-HPAA-Alg-Chi solution might be due to the synergistic effect of 3-HPAA, alginate-chitosan, and acetic acid. It is clear that the 3-HPAA-Alg-Chi nanoparticles have bacteriocidal effects on pathogenic bacteria regardless of being Gram-negative or Gram-positive. The application concentration of the nanoparticle solution should be determined for model systems for future usage.

4. Conclusions

In the current study, we have reported the synthesizing homogeneous nanoparticles made up of alginate and chitosan polymers loaded with 3-HPAA with very high encapsulation percentage and antimicrobial properties. Additionally, we have suggested the proper usage conditions of them as antimicrobial agents against four of the most important nosocomial pathogens. Since our main purpose was to generate a nanoparticle solution with a high antimicrobial effect, the nanoparticle solutions were tested in volume/volume concentrations by applying acetic acid with a very low concentration (1% in ddH_2O) to provide pH change. To conclude;

• Usage of the crosslinkers in higher concentrations (such as 25 mM of $CaCl_2$) in the production process of alginate-chitosan nanoparticles results in the synthesis of smaller nanoparticles with very high homogeneity and very high encapsulation percentage of simple phenolic acid.

• Both 24 hours and 72 hours of 1% (v/v, in ddH2O) acetic acid treatment of 3-HPAA-Alg-Chi before their usage in the antimicrobial tests results in a similar antimicrobial pattern. Thus, the stock 3-HPAA-Alg-Chi solution can be used as an antimicrobial agent after 24 hours of 1% acetic acid treatment as well as after 72 hours of the treatment.

• Although 10% (v/v) usage of the 3-HPAA-Alg-Chi nanoparticle solution in 1% acetic acid showed the bacteriocidal effect on *P. aeruginosa* and *S. epidermidis*, it was bacteriostatic on MRSA and MSSA. Thus, 20% (v/v) of 3-HPAA-Alg-Chi nanoparticle solution in 1% acetic acid is required to obtain the bacteriocidal effect on both MRSA and MSSA.

• The Alg-Chi nanoparticle solutions loaded with 3-HPAA showed the bacteriocidal effect on each bacterium with the bacterial load of 10^6 cfu/ml, which is a very high bacterial load. Therefore, this nanoparticle solution would be much more effective on the nosocomial bacteria with lower bacterial load, which is the case in most nosocomial

infections.

• Even though different concentrations were required, the nanoparticle solution had bacteriocidal effects on tested nosocomial bacteria, regardless of their cell wall properties. Therefore, the 3-HPAA-Alg-Chi solution is a promising antimicrobial agent that can be used against microbial pathogenesis in the future.

To sum up, 3-HPAA loaded alginate-chitosan nanoparticle solution can be presented as a succeeding antimicrobial agent for combatting or preventing the infections caused by *P. aeruginosa* and *Staphylococci*.

Acknowledgments

We would like to thank "Izmir Institute of Technology, Biotechnology and Bioengineering Research and Application Center" and "Izmir Institute of Technology, Center for Materials Research". This work was funded by Izmir Institute of Technology Research Fund by Project # 2014IYTE22.

References

Azevedo, M.A., Bourbon, A.I., Vicente, A.A. and Cerqueira, M.A. (2014), "Alginate/chitosan nanoparticles for encapsulation and controlled release of vitamin B2", *Int. J. Biol. Macromol.*, **71**, 141-146. https://doi.org/10.1016/j.ijbiomac.2014.05.036.

Barrera-Necha, L.L., Correa-Pacheco, Z.N., Bautista-Baños, S., Hernández-López, M., Jiménez, J.E.M. and Mejía, A.F.M. (2018), "Synthesis and characterization of chitosan nano-particles loaded botanical extracts with antifungal activity on Colletotrichum gloeosporioides and Alternaria species", *Adv. Microbiol.*, **8**(4), 286-296. https://doi.org/10.4236/aim.2018.84019.

Budnyak, T.M., Yanovska, E.S., Kichkiruk, O.Yu., Sternik, D. and Tertykh V.A. (2016), "Natural minerals coated by biopolymer chitosan: Synthesis, physicochemical, and adsorption properties", *Nanosc. Res. Lett.*, **11**(1), 1-12. http://doi.org/10.1186/s11671-016-1752-7.

Cueva, C., Moreno-Arribas, M.V., Martín-A´ lvarez, P.J., Bills, G., Vicente, M.F., Basilio, A., Rivas, C. L., Requena, T., Rodríguez, J.M. and Bartolome´, B. (2010), "Antimicrobial activity of phenolic acids against commensal, probiotic and pathogenic bacteria", *Res. Microbiol.*, **161**(5), 372-382. https://doi.org/10.1016/j.resmic.2010.04.006.

Deka, C., Deka, D., Bora, M.M., Jha, D.K. and Kakati, D.K., (2016), "Synthesis of peppermint oil-loaded chitosan/alginate polyelectrolyte complexes and study of their antibacterial activity", *J. Drug Deliv. Sci. Tech.*, **35**, 314-322. https://doi.org/10.1016/j.jddst.2016.08.007.

Díaz-Gómez, R., López-Solís, R., Obreque-Slier, E. and Toledo-Araya, H. (2013), "Comparative antibacterial effect of gallic acid and catechin against Helicobacter pylori", *LWT Food Sci. Technol.*, **54**(2), 331-335. https://doi.org/10.1016/j.lwt.2013.07.012.

Gutiérrez-Larraínzar, M., Rúa, J., Caro, I., de Castro, C., de Arriaga, D., García-Armesto, M.R. and del Valle, P. (2012), "Evaluation of antimicrobial and antioxidant activities of natural phenolic compounds against foodborne pathogens and spoilage bacteria", *Food Control*, **26**(2), 555-563. https://doi.org/10.1016/j.foodcont.2012.02.025.

Hurtado-Fernandez, E., Gomez-Romero, M., Carrasco-Pancorbo, A. and Fernandez-Gutierrez, A. (2010), "Application and potential of capillary electro separation methods to determine antioxidant phenolic compounds from plant food material", *J. Pharmaceut. Biomed.*, **53**(5), 1130-1160. https://doi.org/10.1016/j.jpba.2010.07.028.

Jamil, B., Habib, H., Abbasi, S., Nasir, H., Rahman, A., Rehman, A., Bokhari, H. and Imran, M. (2015), "Cefazolin loaded chitosan nanoparticles to cure multi drug resistant Gram-negative pathogens", *Carbohyd. Polym.*, **136**, 682-691.

Jamil, B., Abbasi R., Abbasi S., Imran, M., Khan, S.U., Ihsan, A., Javed, S., Bokhari, H. and Imran M. (2016), "Encapsulation of cardamom essential oil in chitosan nano-composites: In-vitro efficacy on antibiotic-resistant bacterial pathogens and cytotoxicity studies", *Front. Microbiol.*, **7**, 1580. https://doi.org/10.3389/fmicb.2016.01580.

Jayakumar, R., Menon, D., Manzoor, K., Nair, S.V. and Tamura H. (2010), "Biomedical applications of chitin and chitosan based nanomaterials-A short review", *Carbohyd. Polym.*, **82**(2), 227-232. https://doi.org/10.1016/j.carbpol.2010.04.074.

Ji, M., Sun, X., Guo, X., Zhu, W., Wu, J., Chen, L., Wang, J., Chen, M., Cheng, C. and Zhang, Q. (2019), "Green synthesis, characterization and in vitro release of cinnamaldehyde/sodium alginate/chitosan nanoparticles", *Food Hydrocolloid*, **90**, 515-522. https://doi.org/10.1016/j.foodhyd.2018.12.027.

Karaosmanoglu, H., Soyer, F., Ozen, B. and Tokatli, F. (2010), "Antimicrobial and antioxidant activities of Turkish extra virgin olive oils", *J. Agr. Food Chem.*, **58**(14), 8238-8245. https://doi.org/10.1021/jf1012105.

Kaur, J., Kour, A., Panda, J.J., Harjai, K. and Chhibber, S. (2020), "Exploring endolysin-loaded alginate-chitosan nanoparticles as future remedy for Staphylococcal Infections", *AAPS Pharm. Sci. Tech.*, **21**(6), 1-15. https://doi.org/10.1208/s12249-020-01763-4.

Khan, F., Manivasagan, P., Pham, D.T.N., Oh, J., Kim, S.K. and Kim, Y.M. (2019), "Antibiofilm and antivirulence properties of chitosan-polypyrrole nanocomposites to *Pseudomonas aeruginosa*", *Microbial Pathogenesis*, **128**, 363-373. https://doi.org/10.1016/j.micpath.2019.01.033.

Krausz, A.E., Adler, B.L., Cabral, V., Navati, M., Doerner, J., Charafeddine, R.A., Chandra, D., Liang, H., Gunther, L., Clendaniel, A., Harper, S., Friedman, J.M., Nosanchuk, J.D. and Friedman, A.J. (2015), "Curcumin encapsulated nanoparticles as innovative antimicrobial and wound healing agent", *Nanomed. Nanotechnol. Biol. Med.* **11**(1), 195-206. https://doi.org/10.1016/j.nano.2014.09.004.

Longuinho, M.M., Leitao, S.G., Silva, R.S.F., Silva, P.E.A., Rossi, A.L. and Finotelli, P.V. (2019), "Lapazine loaded Alginate/ Chitosan microparticles: Enhancement of anti-mycobacterium activity", *J. Drug Deliv. Sci. Tech.*, **54**, 101292. https://doi.org/10.1016/j.jddst.2019.101292.

Li, Z., Jiang, H., Xu, C. and Gu, L. (2015), "A review: Using nanoparticles to enhance absorption and bioavailability of phenolic phytochemicals", *Food Hydrocolloid*, **43**, 153-164. https://doi.org/10.1016/j.foodhyd.2014.05.010.

Liu, J., Xiao, J., Li, F., Shi, F., Li, D. and Huang, Q. (2018), "Chitosan-sodium alginate nanoparticle as a delivery system for ε-polylysine: Preparation, characterization and antimicrobial activity", *Food Control*, **91**, 302-310. ttps://doi.org/10.1016/j.foodcont.2018.04.020.

Madureira, A.R., Pereira, A., Castro, P.M. and Pintado, M. (2015), "Production of antimicrobial chitosan nanoparticles against food pathogens", *J. Food Eng.*, **167**, 210-216. https://doi.org/10.1016/j.jfoodeng.2015.06.010.

Mladenovska, K., Cruaud, O., Richomme P., Belamie, E., Raicki, R.S., Venier-Julienne, M.C., Popovski, E., Benoit, J.P. and Goracinova, K. (2007), "5-ASA loaded chitosan-Ca-alginate microparticles: Preparation and physicochemical characterization", *Int. J. Pharm.*, **345**(1-2), 59-69.

https://doi.org/10.1016/j.ijpharm.2007.05.059.
Mohammadi, A., Hashemi, M. and Hosseini, S.M. (2016), "Effect of chitosan molecular weight as micro and nanoparticles on antibacterial activity against some soft rot pathogenic bacteria", *LWT Food Sci. Technol.*, **71**, 347-355. https://doi.org/10.1016/j.lwt.2016.04.010
Moschona, A. and Liakopoulou-Kyriakides, M. (2018), "Encapsulation of biological active phenolic compounds extracted from wine wastes in alginate-chitosan microbeads", *J. Microencapsul.*, **35**(3), 229-240. https://doi.org/10.1080/02652048.2018.1462415.
MubarakAli, D., LewisOscar, F., Gopinath, V., Alharbi, N.S., Alharbi, S.A. and Thajuddin, N. (2018), "An inhibitory action of chitosan nanoparticles against pathogenic bacteria and fungi and their potential applications as biocompatible antioxidants", *Microb. Pathogenesis*, **114**, 323-327. https://doi.org/10.1016/j.micpath.2017.11.043.
Paques, J.P., van der Linden, E., van Rijn, C.J.M. and Sagis, L.M.C. (2014), "Preparation methods of alginate nanoparticles", *Adv. Colloid Interfac.*, **209**, 163-171. https://doi.org/10.1016/j.cis.2014.03.009.
Nalini, T., Basha, S.K., Sadiq, A.M.M., Kumari, V.S. and Kaviyarasu, K. (2019), "Development and characterization of alginate/chitosan nanoparticulate system for hydrophobic drug encapsulation", *J. Drug Deliv. Sci. Tech.*, **52**, 65-72. https://doi.org/10.1016/j.jddst.2019.04.002.
Qi, L., Xu, Z., Jiang, X., Hu, C. and Zou, X. (2004), "Preparation and antibacterial activity of chitosan nanoparticles", *Carbohyd. Res.*, **339**(16), 2693-2700. https://doi.org/10.1016/j.carres.2004.09.007.
Scolari, I.R., Paez, P.L., Musri, M.M., Petiti, J.P., Torres, A. and Granero, G.E. (2020), "Rifampicin loaded in alginate/chitosan nanoparticles as a promising pulmonary carrier against *Staphylococcus aureus*", *Drug Deliv. Translat. Res.*, **10**, 1403-1417. https://doi.org/10.1007/s13346-019-00705-3.
Supraja, N., Avinash B. and Prasad, T.N.V.K.V. (2017), "*Nelumbo nucifera* extracts mediated synthesis of silver nanoparticles for the potential applications in medicine and environmental remediation", *Adv. Nano Res.*, **5**(4), 373-392. http://doi.org/10.12989/anr.2017.5.4.373.
Supraja, N., Dhivya, J., Prasad T.N.V.K.V. and David E. (2018), "Synthesis, characterization and dose dependent antimicrobial and anticancerous efficacy of phycogenic (*Sargassum muticum*) silver nanoparticles against Breast Cancer Cells (MCF 7) cell line", *Adv. Nano Res.*, **6**(2), 183-200. http://doi.org/10.12989/anr.2018.6.2.183.
Tang, D.W., Yu, S.H., Ho, Y.C., Huang, B.Q., Tsai, G.J., Hsie, H.Y., Sung, H.W. and Mi, F.L. (2013), "Characterization of tea catechins-loaded nanoparticles prepared from chitosan and an edible polypeptide", *Food Hydrocolloid*, **30**(1), 33-41. https://doi.org/10.1016/j.foodhyd.2012.04.014.
Vizhi, D.K., Supraja, N., Devipriya, A., Tollamadugu, N.V.K.V.P and Babujanarthanam, R. (2016), "Evaluation of antibacterial activity and cytotoxic effects of green AgNPs against Breast Cancer Cells (MCF 7)", *Adv. Nano Res.*, **4**(2), 129-143. http://doi.org/10.12989/anr.2016.4.2.129.
Wu, T., Li, Y., Shen, N., Yuan, C. and Hu, Y. (2018), "Preparation and characterization of calcium alginate-chitosan complexes loaded with lysozyme", *J. Food Eng.*, **233**, 109-116. https://doi.org/10.1016/j.jfoodeng.2018.03.020.
Yang, J.S., Xie, Y.J. and He, W. (2011), "Research progress on chemical modification of alginate: A review", *Carbohyd. Polym.*, **84**(1), 33-39. https://doi.org/10.1016/j.carbpol.2010.11.048.